ingegneria sismica
International Journal of Earthquake Engineering
Anno XLIII - Num. 3 - 2026

Application of an Oblique-Photogrammetry-Based BIM Model in High-Slope Excavation

Zhaozuo Zhang[1,*]

[1] Industrial and Civil Engineering, Changsha Railway University, Changsha, 410000, Hunan, China

SUMMARY: *High-slope excavation in railway hub projects needs to achieve stable terrain reconstruction, defensible earthwork calculations, and visual coordination of design with construction. High-slope excavation on the south side of the Shenshan Station Hub Project was selected as the engineering case for this study to develop an integrated oblique-photogrammetry and BIM workflow. Low-altitude UAV oblique images were acquired with 80% forward overlap, 70% side overlap, a relative flight height of 150 m, a 1:500 mapping scale, and an approximate ground sampling distance of 3 cm. Aerotriangulation, dense matching, point-cloud cleaning, semantic segmentation, terrain-surface reconstruction, Civil 3D slope design, Dynamo-assisted quantity extraction and Revit-based model coordination were all performed on the image block. To strengthen the computational basis of the original study, this revision adds ground sampling distance, overlap-control, terrain-difference volume, cross-section volume, relative-deviation, vertical accuracy and progress-control formulas. As shown in the case comparison, the field-survey section method had an excavation volume of 193,899 m³, and the oblique-photogrammetry-BIM workflow had an excavation volume of 188,457 m³. The absolute difference is 5,442 m³ and the relative deviation is 2.81%; both are within the engineering control limit of 3%. The revised workflow now clarifies how the slope crest line, toe line, staged excavation surface and coordination model are derived from the same spatial data source. Based on the above research, it can be seen that the combination of oblique photogrammetry and BIM can improve the traceability of high-slope design, reduce manual interpretation in irregular terrain, and support visual construction briefings, quantity verification and risk-controlled excavation management.*

KEYWORDS: *high slope; oblique photogrammetry; BIM; UAV; earthwork calculation; Civil 3D; railway hub*

1 Introduction

High-slope excavation is still a high-risk construction activity in the railway hub project because many design limits, ground conditions, bridge clearances, haulage routes and support steps are interconnected in three dimensions. Traditional design work has been based on manual topographic surveys and two-dimensional drawings. Although this way can still meet the demands of simple terrain, it is not feasible when the excavation boundary passes through an irregular mountain area that has already undergone previous construction. At this time, the slope crest line is not easy to ascertain from contour drawings alone; the quantity boundary shifts with adjustments to the design surface, and the construction team cannot see spatially

*15732113284@163.com
https://doi.org/10.65102/is20261274
Published: 10 June, 2026

how the mountain mass, bridge structure, working platform, and staged slope surface are interconnected. Research on construction resources shows that BIM-GIS-IoT integration seeks to connect spatial geometry with quantitative construction data for an auditable foundation of resource monitoring and management [1].

Therefore, the application problem of this case is not only model visualisation. The Design Team needs to obtain a reliable terrain surface, convert it into a BIM-compatible engineering object, set slope parameters according to geological and bridge-clearance constraints, calculate excavation quantities, compare the result with field-survey measurements, and present the staged scheme to construction participants. BIM and GIS have been applied to digitise the built environment and link engineering models with geospatial information more and more frequently [2]. Only if the model can guarantee the consistency of coordinates for field acquisition and earthwork calculations will it be suitable for high-slope excavation. A visually appealing model that is not in a controlled coordinate system cannot be used for quantity verification or construction decisions.

Road and Railway Infrastructure Projects introduce additional limitations to model integration. The space-time relation between the linear structure and the ground is often elongated, the right-of-way is narrow, and the excavation surface needs to be coordinated with bridge foundations, temporary roads, drainage, retaining works and mechanical access. BIM-GIS integration has been proposed as a technical foundation for intelligent road management, and civil assets need to be interpreted in relation to a georeferenced corridor rather than as isolated buildings [3]. The Shenshan Station case has the same corridor features: the south-side mountain mass is in conflict with the bridge alignment, and excavation must be controlled to maintain construction access and safety.

UAV oblique photogrammetry can be used to acquire field data for the above-ground structure. UAV images can record the continuous surface in inaccessible or unsafe slope areas more conveniently than ground surveys with total stations or GNSS point collections. Based on the reviews of UAV applications in construction management, UAVs are used for surveying, progress monitoring, safety inspection and digital-site documentation; however, the reliability of the output is still affected by flight design, image overlap, camera geometry, ground-control/check information and post-processing quality [4]. The above factors directly affect the reconstructed terrain surface and, as a result, the calculated cut volume in slope excavation.

Based on the above monitoring and inspection studies, it can be seen that UAVs are more beneficial when their outputs directly inform construction-control decisions, rather than merely serving as visual record-keeping tools [5]. A UAV-based model is constructed in this study to drive the design of an excavation surface and is not used solely as a site image. The surface is imported into Civil 3D, and then the original mountain surface and the designed slope surface are compared to obtain the cut volume. Thus, it can be seen how the survey data relates to the actual quantity in the workflow more directly than when the images, sections and quantity sheets are managed separately.

Reviews of applications for photogrammetry and LiDAR indicate that, in order to be used as reliable engineering input, three-dimensional point clouds need to be filtered, segmented, resampled, and validated in coordinate system [6]. Therefore, the current revision adds specific computational formulas, quality-control indicators, introductions to figures and tables, and post-figure interpretations to the original technical description. The three contributions of the revised manuscript are: first, to build an end-to-end oblique-photogrammetry-BIM workflow for high-slope excavation; second, to convert the original empirical comparison into quantitative verification with deviation calculation; and third, to replace domestic Chinese references with international sources cited once in sequence.

2 Project Introduction

The five above-ground floors and one basement of the Shenshan Station high-speed railway hub complex are as follows. On the south side of the project, the main bridge of the Shenshan Line interferes with an existing mountain body. The surface of the mountain is uneven because a section of the slope has been excavated previously; thus, there are irregular local benches, discontinuous exposed areas, and an unclear slope boundary. The initial site condition obtained by UAV is shown in Figure 1. Therefore, the figure is selected as the starting point for the digital workflow to show why only traditional two-dimensional contour interpretation is insufficient to determine the excavation boundary accurately.

Figure 1: *Drone image of the South-side Mountain and Planned Excavation Area*

As shown in Figure 1, the excavation object is not a regular embankment or a simple borrow pit. The bridge alignment, local terrain relief, vegetation, and disturbed ground surface are all different shapes. For the calculation of quantity, one must establish a continuous original terrain surface and then subtract the designed excavation surface under the same coordinate system. The above requirement is the reason for using oblique photogrammetry as the starting data source.

The Design scheme uses multiple high-slope sections to avoid the bridge conflict and meet the site-platform requirements. The top and bottom of the excavation are at 8.00 m and 54.42 m, and the total vertical distance is about 45 m. Set up five slope stages. The upper first-stage slope has relatively poor ground conditions and will be constructed at a slope ratio of 1:2, while the lower fifth-stage slope has good geology and will be built at a slope ratio of 1:1.25. The intermediate slope ratios are reduced by 0.25 at each step in the engineering design. A typical cross-section is shown in Figure 2.

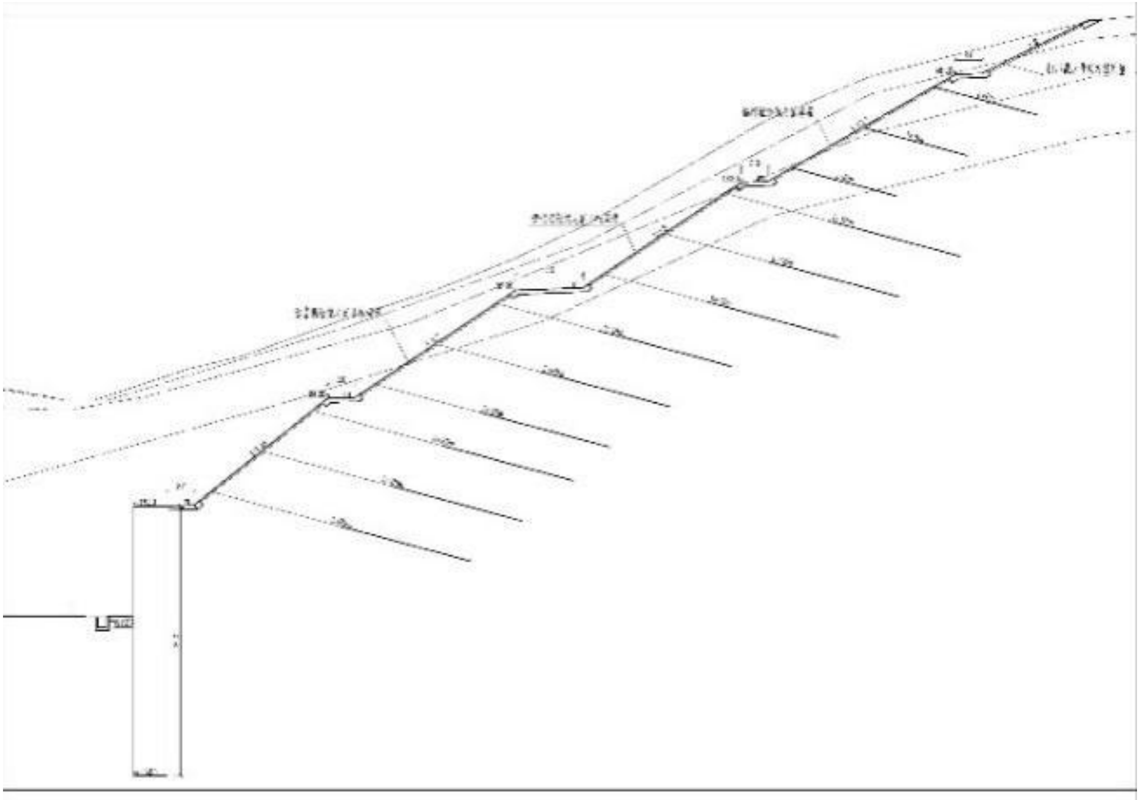

Figure 2: Typical cross-section of the designed high-slope

Figure 2 is the design-control geometry in the BIM modelling stage. The staged slope is not for decoration; rather, it is used to set the breakline that controls the design surface, as well as the positions of the crest and toe, and the final excavation boundary. When these lines are projected onto an uneven oblique-photogrammetry surface, even small differences in the local elevation of the ground can result in a relatively large total error of the cut volume. Therefore, the cross-section should be converted into a parametric design surface and no longer used as a static drawing.

The space conflict of the mountain body and the bridge structure is shown in Figure 3. The model view is more intuitive for displaying the excavation objectives than a plan or section; that is to say, a controlled boundary should be set to remove a mountain mass, and enough space needs to be preserved for the bridge and future station facilities.

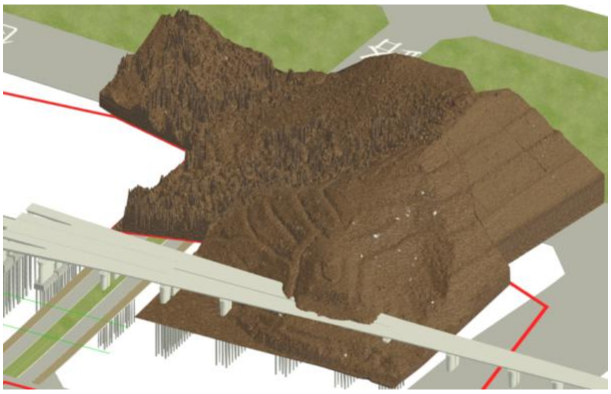

Figure 3: Spatial Relationship of the Mountain Mass and the Bridge Structure

Figure 3 shows that the amount of money needs to be related to the bridge model and the planned construction platform. If the excavation surface is calculated separately from the bridge model, although a design that looks reasonable in section may still result in local clearance conflicts or construction-access problems. Therefore, the revised workflow will now treat earthwork calculation and BIM coordination as a single modelling chain.

3 Methods

3.1 Integrated Technical Route

The first stage of the technical route sets up the site and ends with the final amount and construction instruction approval. To avoid the loose sequence of independent software operations, a single coordinate-controlled data path is used for the entire workflow: UAV image acquisition → aerotriangulation → dense point-cloud generation → point-cloud cleaning → terrain modelling → rightarrow → slope design → volume calculation → BIM coordination. Figure 4 shows the revised English technical route.

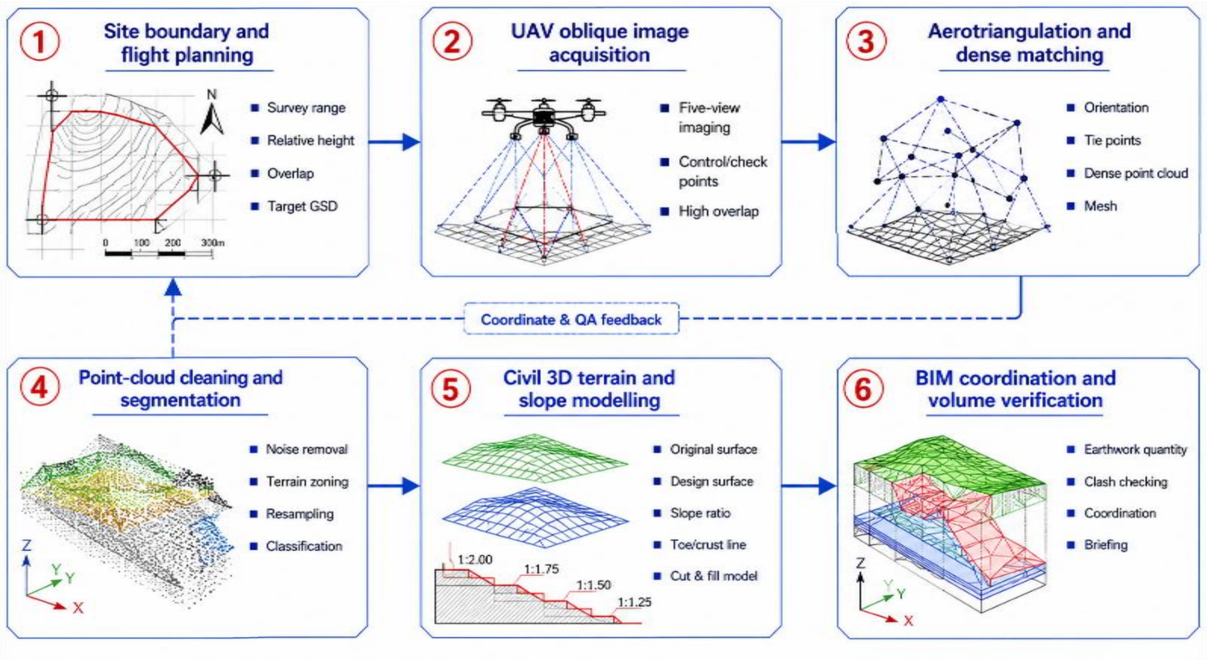

Figure 4: Technical Route of UAV Oblique Photogrammetry and BIM-based Excavation Modelling

Figure 4 shows the purposes of the different digital objects. The UAV image block provides the original spatial information; a dense point cloud serves as the foundation for reconstruction; Civil 3D creates an engineering surface from the point cloud, and Revit is coordinated with other disciplines in the project. The coordinate and quality-control feedback loop is introduced to avoid errors in acquisition or reconstruction from spreading to slope-line extraction and earthwork statistics. The revised workflow is no longer a black box, and the calculation stage will be linked to the measurement parameters and geometric formulas listed below.

3.2 UAV Data Acquisition and Photogrammetric Control

Oblique photogrammetry will be employed for the collection of data. A multi-lens UAV sensor acquires one nadir image and four oblique images during flight to obtain data on the terrain surface, exposed slope faces, local benches and adjacent structures from multiple directions. A target Area of available base map and site survey has been selected before the take-off. The planned route will cover the entire mountain body, the bridge-interference zone, the planned platform boundary, and an adequate surrounding buffer for model reconstruction.

The chosen flight parameters met the engineering-level requirements for topographic mapping in this case: 80% forward overlap, 70% side overlap, 150m relative flight height, 1:500 mapping scale, and approximately a ground sampling distance of 3cm. These parameters have been extracted from the original paper and now correspond to explicit control equations. The approximate ground sampling distance can be expressed as Equation (1), and H is the relative flight height, p is the camera pixel size, and f is the camera focal length.

$$GSD = (H \times p)/f \tag{1}$$

The overlap setting controls the geometric strength of image matching and aerotriangulation. For a simplified image footprint with ground length L and width W, the forward base Bf and side base Bs should satisfy Eq. (2) and Eq. (3). These formulas explain why the route in this case used high overlap: the mountain surface contains vegetation, local shadow, and irregular slope faces, which require sufficient tie-point redundancy for stable reconstruction.

$$Of = 1 - Bf/L \tag{2}$$

$$Os = 1 - Bs/W \tag{3}$$

Table 1 shows the fixed acquisition and processing parameters before the earthwork calculation. A table has been added to enable verification of the method and prevent the model from being a general description of software.

Table 1: UAV Acquisition and Processing Control Parameters

Control item	Value or software	Role in the workflow	Risk controlled
Forward overlap	80%	Improves tie-point redundancy along flight direction	Image matching failure and weak geometry
Side overlap	70%	Maintains cross-strip coverage for oblique views	Surface gaps and discontinuous reconstruction
Relative flight height	150 m	Controls image footprint and GSD	Low-resolution terrain surface
Mapping scale	1:500	Sets engineering-grade mapping target	Quantity calculation from coarse terrain
Ground sampling distance	Approx. 3 cm	Defines surface detail captured by each pixel	Loss of local benches and slope breaks
Photogrammetry software	ContextCapture	Aerotriangulation, dense matching, and GIS model output	Uncontrolled image geometry
Point-cloud processing	CloudCompare	Noise removal, segmentation, and resampling	Excessive point density and vegetation noise
Engineering modelling	Civil 3D, Dynamo, Revit	Surface generation, volume extraction, BIM coordination	Disconnected quantity and coordination models

As shown in Table 1, the parameters of the field survey, point cloud processing and BIM modelling are all related to an objective function. Thus, the method is reproducible at the engineering level, and another project can change the flight height, overlap, ground-control layout and resampling density while using the same computation logic.

3.3 Construction of the Real-Scene Model and Accuracy Indicators

ContextCapture is employed to process the original UAV images. First, the image block is aerotriangulated and then bundle adjusted. Homologous image points were extracted from several photographs to determine the exterior orientation parameters of each image and to build a geometric topology of the photographs. Aerotriangulation is then performed to check for image coverage, projection-center distribution, camera attitude, overlap completeness and sparse point-cloud consistency in the software. Then, dense matching was used to obtain a high-density 3D point cloud and a textured mesh model. Research on UAV-based earthwork volume calculation shows that the value of UAV surveying depends on how precisely a photogrammetric surface can be converted into a reliable volume boundary [7].

For quality control, the vertical accuracy of the reconstructed terrain can be evaluated by the root mean square error shown in Eq. (4), where zi is the surveyed elevation of an independent check point, zhat_i is the elevation extracted from the reconstructed surface at the same location, and n is the number of check points. The original project record did not report independent check-point residuals; therefore, Eq. (4) is added as a required verification index for future repeated use of the method.

$$\mathrm{RMSE}_z = \sqrt{\frac{1}{n}\sum_{i=1}^{n}(z_i - \hat{z}_i)^2} \tag{4}$$

The reconstructed GIS terrain model is as follows: Figure 5. Retain the spatial geometry and orthophoto texture to help the engineering team conduct an inspection for continuity problems in the terrain, steep local breaks, model voids, etc., before importing the surface data into the following BIM software.

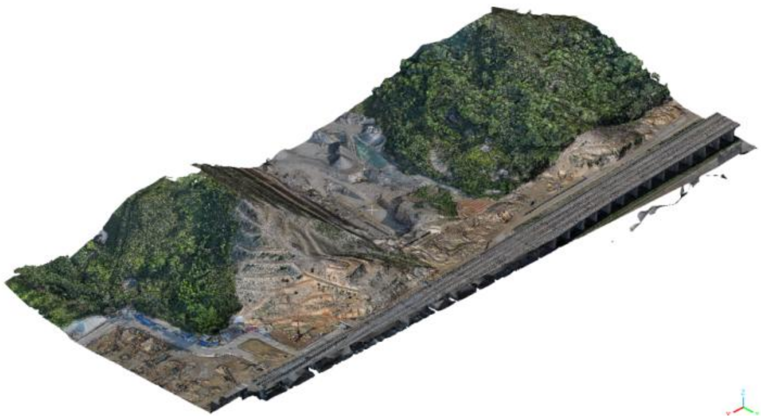

Figure 5: Terrain model generated by UAV oblique photogrammetry

As shown in Figure 5, a real-scene model can be used to present the irregular mountains and their surroundings in a single view. This visual continuity is required to check whether the excavation boundary is within the bridge clearance, construction access areas and the existing disturbed slope. It will be known whether there are areas with dense vegetation or shadows that will reduce the accuracy of the point cloud data.

Generate a GIS model, import the dense point cloud into CloudCompare for semantic segmentation and resampling, etc. Terrain, existing slope faces, vegetation-affected areas and model-noise zones are all segmented. Reduce the size of the point cloud by resampling and maintain breaklines and local relief for earthwork calculations. UAV earthwork studies for road construction also show that the volume results are dependent on the reconstructed terrain surface and the measurement strategy used to define the comparison surface [8].

The result of semantic segmentation is as follows: Figure 6. The revised text will use this figure as a way to show the method-control rather than presenting all of the software output.

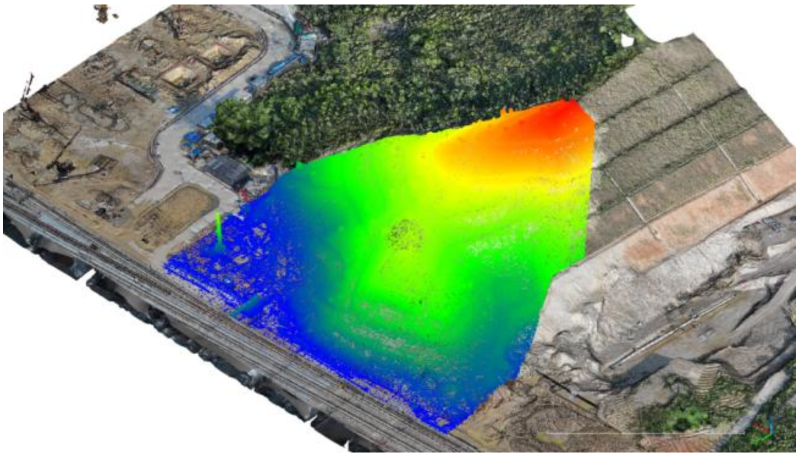

Figure 6: Semantic Segmentation and Surface Zoning of the Terrain Model

Figure 6 shows that the point cloud was processed before Civil 3D modelling. Thus, the data volume is reduced and non-terrain points will not be included in the surface model. A steep slope will directly affect the crest-line projection and the final volume of the slope in areas with vegetation or shade.

3.4 BIM Terrain Modelling and Earthwork Calculation

Export and import the cleaned point cloud into Civil 3D to create the original mountain terrain surface. Civil 3D was then used to set the designed platform elevation, slope ratios, slope stages, and the relationship between the original terrain and the designed excavation surface. The Terrain-Surface generation process is as follows: Figure 7.

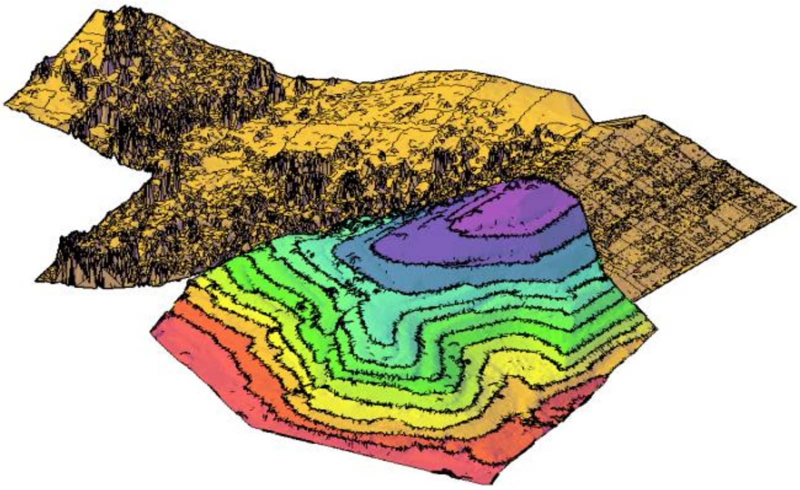

Figure 7: Terrain Surface Generated in Civil 3D from Processed Point Cloud Data

Fig. 7 shows the conversion from measured point data to an engineering surface. The role of Civil 3D is to transform the real-scene point cloud into a triangulated terrain surface that can receive design parameters. The slope ratio is expressed in this manuscript as Eq. (5), where m is the horizontal-to-vertical slope coefficient, Δx is the horizontal distance, and Δz is the vertical rise. For a slope ratio of 1:m, the slope angle θ is obtained by $\arctan\left(\frac{1}{m}\right)$.

$$m = \frac{\Delta x}{\Delta z}, \qquad \theta = \arctan\left(\frac{1}{m}\right) \tag{5}$$

The design surface is generated by projecting the staged slope parameters onto the original terrain. Earthwork is obtained by comparing the original terrain elevation $z_0(x, y)$ with the design terrain elevation $z_d(x, y)$ over the computational area A. The continuous cut and fill quantities are described by Eq. (6). In the present case, the main concern is excavation, but the fill term is retained for completeness because the same workflow can be used for platform levelling or roadbed balancing.

$$V_{\text{cut}} = \iint_A \max[z_0(x,y) - z_d(x,y), 0]\, dA, \qquad V_{\text{fill}} = \iint_A \max[z_d(x,y) - z_0(x,y), 0]\, dA \tag{6}$$

For numerical computation, the surface difference can be discretized by grid cells or triangulated irregular network elements. The corresponding approximation is given in Eq. (7), where ΔA_i is the local cell or triangular element area and N is the number of elements. This formula links the model-based result with a reproducible geometric calculation rather than treating the BIM output as an unexamined software number.

$$V_{\text{cut}} \approx \sum_{i=1}^{N} \max\left(z_{0,i} - z_{d,i}, 0\right)\Delta A_i, \qquad V_{\text{fill}} \approx \sum_{i=1}^{N} \max\left(z_{d,i} - z_{0,i}, 0\right)\Delta A_i \tag{7}$$

The final Civil 3D excavation model is as follows: Figure 8. The model is the designed excavation body, and Dynamo-assisted quantity extraction is based on this model.

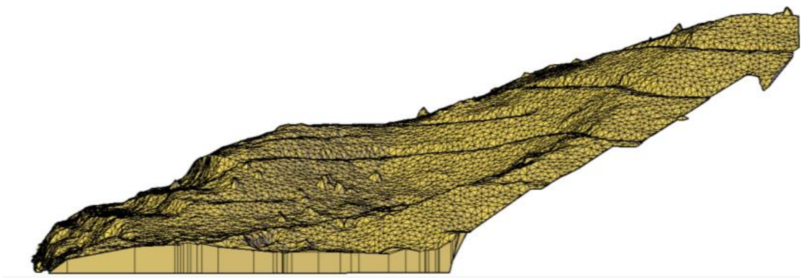

Figure 8: Civil 3D Earthwork Excavation Model for the High-Slope Area

Figure 8 is the engineering output of the workflow. The body of the excavation is no longer inferred from isolated sections; instead, it is obtained by analysing the three-dimensional terrain surface measurement and the design of the slope surface. Therefore, the computed volume is more susceptible to fluctuations in the local ground conditions; this is precisely the reason for the uncertainty in the old section method.

3.5 Fusion Platform and Model Coordination

Import the original terrain model and the design excavation model into Revit for integrated BIM work. Align the BIM project's base point with the coordinate system of the photogrammetry-derived model before model fusion. Otherwise, the BIM model would not be properly positioned in relation to terrain and bridge data for comparison. Alignment can then be carried out for three-dimensional interference checks, platform clearance analysis, construction access planning and technical briefings.

A Revit Coordination Environment was employed to obtain the location and attribute data of the components. A model-based communication function for the owner, designer, contractor and supervisor in slope excavation. The same integrated model can be used to present the planned excavation order, support installation sequence, temporary road layout, machine working areas and local safety risks. Therefore, the revised manuscript will no longer present BIM coordination as a final display effect but as a construction control step.

4 Application Results and Verification

4.1 Comparison of Section Measurement and Oblique Photogrammetry-BIM Calculation

The original project compared two calculation methods: the field-survey section method and the oblique-photogrammetry-BIM method. The section method uses measured cross-sections and computes volume from adjacent section areas. Its basic calculation is expressed in Eq. (8), where A_k and A_{k+1} are the cut areas of two adjacent sections and L_k is the distance between them. The method can produce reasonable results for linear works, yet its accuracy depends heavily on section spacing and manual modification where the design surface is irregular.

$$V_{\text{sec}} = \sum_{k=1}^{n-1} \frac{A_k + A_{k+1}}{2} L_k \tag{8}$$

The oblique-photogrammetry-BIM result was compared with the field-survey result by relative deviation, as shown in Eq. (9). V_{survey} denotes the excavation quantity obtained from the field-survey section method, and V_{BIM} denotes the excavation quantity obtained from the oblique-photogrammetry-BIM workflow.

$$\delta = \frac{|V_{\text{BIM}} - V_{\text{survey}}|}{V_{\text{survey}}} \times 100\% \tag{9}$$

Table 2 shows the revised calculation comparisons. The original table had a 3% discrepancy. Add the absolute difference and the recalculated relative deviation to make the result more explicit in this revision.

Table 2: Comparison of excavation quantity calculation results.

Calculation method	Total earthwork volume (m³)	Excavation volume (m³)	Absolute difference from field survey (m³)	Relative deviation
Field-survey section method	-	193,899	-	-
Oblique-photogrammetry-BIM method	349,023	188,457	5,442	2.81%
Engineering control interpretation	Not directly comparable with section total	Comparable excavation quantity	Within the 3% control threshold	Rounded as 3.0%

As shown in Table 2, the difference in the two excavation quantities is 5,442 m³, which is 193,899 m³ - 188,457 m³. The relative deviation is 2.81%; it will be rounded to 3.0% in the engineering statement. The total earthwork volume of 349,023 m³ obtained from the photogrammetry-BIM workflow should not be directly compared with the field-survey excavation value because they have different scopes of quantity. The comparable index is the excavation volume, and the model-based result remains within the set control range.

The most typical case of the value of model-based methods is an irregular mountain area. Although a section method can be adopted to reduce the distance between sections, the work done in the field will be larger, and handling of uneven surfaces will still need to be done manually. Oblique Photogrammetry - BIM is used to generate continuous surface models for parametrically adjustable Design Slopes. Forest-road studies have also reported that UAV-based surfaces can support volume estimation for earthwork operations when the terrain change is represented continuously rather than by a few profiles [9].

4.2 Comparison of Methods and Engineering Interpretation

Assess the two methods by the quantity of data, accessibility of terrain, model reuse and construction coordination. Table 3 is an expansion of the original comparison and, therefore, does not need to be referred to in the results section again.

Table 3: Engineering Comparison of the Two Quantity Methods

Comparison item	Field-survey section method	Oblique-photogrammetry-BIM method	Effect on this case
Data density	Discrete points and cross-sections	Continuous image-derived point cloud and terrain surface	Better representation of local benches and irregular slope faces
Terrain accessibility	Unsafe or inaccessible points may be omitted	Remote acquisition covers steep and disturbed zones	Reduces field exposure and missing geometry
Quantity boundary	Manual section editing required when surface changes rapidly	Original and design surfaces intersect directly in Civil 3D	Improves traceability of slope crest and toe lines
Model reuse	Quantity result is separated from coordination model	Surface, excavation body, and BIM coordination model share one chain	Supports briefing, clash review, and construction sequencing
Main limitation	High workload under dense section spacing	Sensitive to vegetation, shadows, GCP/check-point control, and point-cloud filtering	Requires targeted field checks at key boundary zones

As shown in Table 3, although the oblique-photogrammetry-BIM method can achieve quantity traceability, field verification is still required. Therefore, the 2.81% deviation can be attributed to the use of a workflow, and other differences may stem from surface reconstruction errors, vegetation cover, field-section spacing, and different definitions of local terrain change by the two methods. Recent studies combining terrestrial laser scanning and drone-based photogrammetry have also demonstrated that a high density of three-dimensional observations is suitable for volume calculation, but the quality of the results is still restricted by the measurement and registration strategy [10].

4.3 Construction Process Visualization and Stage Briefing

The integrated model was used to visualize the excavation process and support construction briefing. The visualization includes staged excavation order, progressive formation of the slope outline, synchronous installation of support measures such as anchors, cables, and shotcrete, working space for machinery, and temporary access routes. The model also allows the planned excavation quantity to be compared with daily or periodic production data. The cumulative progress index can be expressed by Eq. (10), where V_t is the completed excavation quantity at time t and V_{design} is the planned design excavation quantity.

$$P_t = \frac{V_t}{V_{\mathrm{design}}} \times 100\% \tag{10}$$

For progress control, the planned and actual quantities can be compared using Eq. (11), where $P_{\mathrm{plan},t}$ is the planned progress ratio and $P_{\mathrm{actual},t}$ is the actual progress ratio at the same time point. The signed deviation clarifies whether the excavation is ahead of or behind the planned sequence.

$$\Delta P_t = P_{\mathrm{actual},t} - P_{\mathrm{plan},t} \tag{11}$$

To help the project participants better understand it, make a graph or chart. A two-dimensional drawing can show the final slope section, but it is not convenient to show how the slope will be opened, where equipment will be placed, how a support measure follows the cut face, or which area becomes unsafe at a certain excavation depth. Recently, UAV-based automated earthwork progress monitoring has developed to use image-derived data for comparison with the expected state [12]. The Shenshan Station case follows the same logic at the engineering-practice level and uses a BIM model as a briefing and progress-control object.

A Visual Briefing Can Raise People's Sense of Danger. Before the excavation, a model can be created to identify any conflicts among temporary roads, machinery working areas, support installation, bridge structures, excavation boundaries, etc. At the same time, the latest UAV and field progress data can be used to update the model and compare it with the planned and actual geometry. If the model shows a localized risk of over-excavation or a mismatch between support timing and the excavation stage, then modify the construction sequence before such a site safety incident occurs.

5 Discussion

5.1 Accuracy Sources and Control Points

Based on the revised calculation, the results from oblique-photogrammetry-BIM are close to those obtained in the field-survey section, but these two sets of data should not be considered the same measurement. Section method reduces the terrain to an adjacent profile; the BIM method calculates the difference between two continuous surfaces. Therefore, the 2.81% relative deviation is due to both measurement errors and different methods. In areas with undulations, even a small height error over a wide area can result in a relatively large volume difference. A sparse section layout will not be able to cover local depressions, ridges, or benches of the point cloud surface.

Vegetation is the primary source of error in the UAV-derived surface. If there are bushes, trees or a dense layer of grass on the ground, the photogrammetric point cloud will be a vegetation canopy rather than the actual ground surface. The original conclusion proposed clearing the surface before collection when feasible, and this still holds true. If clearing is not feasible, then use a higher-resolution image, increase the overlap, ensure suitable lighting conditions, and perform targeted total-station or GNSS elevation checks at the key slope boundaries. Accuracy analysis of RTK/PPK UAV photogrammetry studies has also shown that differential correction and control-point methods affect the accuracy of 3D mapping [11].

The other is a simple model. Resampling is needed because the raw dense point cloud may be too large for the downstream BIM software. However, over-resampling will blur the abrupt changes in the ground and move the crest or toe. Therefore, the modified workflow will use semantic segmentation before resampling. Terrain, vegetation, existing structures and noise should be excluded from the area of simplification of the terrain surface, and a regular point-spacing rule cannot be applied uniformly.

5.2 Model Integration and Digital Twin Applications

The present case does not aim to be a complete digital twin, as it does not continuously transmit sensor data to a live numerical model. However, it has built a practical digital foundation for a slope-excavation twin: a coordinate-controlled terrain model, a parametric excavation design surface, a quantity calculation object, and a model-based progress briefing environment. Voxel-based digital twin frameworks for earthwork construction have shown that three-dimensional discretization can support progress comparison and data-driven control of design and actual states in a common spatial model [13].

Geotechnical Excavation still has some uncertainties. There may be measurement residuals on the terrain surface, a simplified geological model, and support timing changes due to site conditions. Probabilistic digital twin research for geotechnical design and construction proposes that when field observations are employed to update design and construction decisions, uncertainty should be explicitly shown [14]. For this type of project, a feasible extension would be to combine the oblique-photogrammetry surface with geological zoning, monitoring points and staged support records to present both the geometry and the risk status of the model.

Maturity of digital applications can also be evaluated by how widely data are used and whether there are decision-support and construction-feedback functions. Quantitative maturity models for underground-infrastructure digital twins require the linking of model data, monitoring data, analysis methods and management decisions [15]. The current process at Shenshan Station for that case has reached model-based surveying, design coordination and quantity verification. A high-maturity level would require regular UAV resurveys, automatic comparison of the design and actual surface, integration of deformation monitoring, and closed-loop adjustment of excavation and support decisions.

5.3 Engineering Applicability and Limitations

A typical situation is a project with rough terrain, a high-risk area for construction access, vague excavation limits, and close proximity to existing buildings. Suitable cases include high-slope excavation next to railway bridges, road cuts in mountainous corridors, large platform levelling, and staged retaining works. This way does not need to be taken for a simple flat-area excavation where a small number of survey points can accurately determine the surface.

The primary deficiency is that a photogrammetry-BIM workflow demands stable data governance. Flight records, camera parameters, ground-control/check data, coordinate transformations, point-cloud filtering settings, Civil 3D surface definitions and quantity reports should all be archived together. If the above materials are not separated, the subsequent reviewers will be unable to replicate the quantity result. Therefore, the revised manuscript will add formulas and control tables not for the sake of theory, but as engineering-traceability documents.

A second deficiency is that the bridge and slope coordination model may not be revised at different times in the design. A modification to the bridge model will need to adjust the excavation area. If the terrain model, slope model and bridge model are not kept in a version control system, the quantity result may not be in line with the latest design. In the future, model versions will be saved along with their dates, coordinate references, software versions, designers and calculation scopes.

Set up a minimum reproducibility package for the project team before the first flight and use it. The package should contain the flight route, image set, camera metadata, coordinate reference, ground-control and check-point records, aerotriangulation report, dense point-cloud file, segmentation rule, resampling setting, original terrain surface, design terrain surface, slope-ratio parameters, quantity report, and the final coordination model. Store the above files under a single model version number. When revising the excavation surface, the previous design surface should not be covered by new construction; otherwise, the difference in quantity cannot be addressed later. The above data governance will help prevent disputes over earthwork quantities that occur after the physical change of the ground in high-slope construction.

Define the boundaries of the new process for engineering data and model analysis. UAV Images and Checkpoints are the evidence. Point cloud cleaning, terrain interpolation, surface triangulation and slope projection are interpretation steps. The calculation report should specify which parts of the model are directly based on field measurements and which parts are produced by design assumptions. To determine if a volume difference results from measurement error, terrain interpolation, design adjustment or a simplified section method, a reviewer can use the above distinctions. Without such separation, the BIM quantity will be accurate but the modelling decisions that led to it cannot be seen.

A BIM model will be used for the site's management and a short calculation audit sheet will be prepared. The audit sheet may contain the acquisition time, weather conditions, flight altitude, overlap, GSD, coordinate system, check-point residual, filtering method, design-surface version, excavation-scope boundary and final quantity. These items are short, but they need to determine whether the model can be used for payment review, technical briefing, safety inspection and later dispute resolution. The added formulas in this revision provide the computational structure for that audit sheet and make the model output easier to verify.

6 Conclusion

This study revises and extends an engineering case on the application of oblique photogrammetry and BIM for high-slope excavation at the Shenshan Station Hub Project. The workflow converts UAV oblique imagery into a GIS terrain model, cleans and segments the point cloud, constructs the original terrain surface in Civil 3D, generates the designed slope surface based on platform elevation and slope-ratio requirements, extracts earthwork quantity, and imports the results into Revit for model coordination and construction briefing.

Based on the case verification, the excavation volume obtained by the field-survey section method was 193,899 m^3, and that of the oblique-photogrammetry-BIM method was 188,457

m^3. The absolute difference is 5,442 m^3 and the relative deviation is 2.81%; 3.0% will be taken for engineering purposes. Therefore, the practical accuracy of the integrated workflow in areas with rough ground has been confirmed, and it is now possible to provide a stable amount for construction management.

The modification adds explicit formulas for ground sampling distance, flight overlap, slope ratio, terrain-difference volume, section-based volume, relative deviation, vertical accuracy and progress-control indicators. The above formulas are more verifiable and less dependent on general-purpose software descriptions. The revision also adds figure lead-ins, post-figure analyses, method-control tables and an international reference list. This way is suitable for the design of high-slope areas, site-level adjustments, road and railway cuts and fills, and earthwork projects that require coordination among terrain measurement, BIM modelling, quantity verification, and visual construction supervision.

Future applications will include independent check-point residuals, periodic UAV re-surveys of the excavation site, terrain-vegetation classification, and model version control. The addition of the above modules will transform the current workflow from a static quantity verification approach into an intelligent closed-loop digital construction management system for complex geotechnical works.

References

[1] Liu X, Antwi-Afari M F, Li J, Zhang Y, Manu P. BIM, IoT, and GIS integration in construction resource monitoring[J]. Automation in Construction, 2025, 174: 106149.

[2] Piras G, Muzi F, Zylka C. Integration of BIM and GIS for the digitization of the built environment[J]. Applied Sciences, 2024, 14(23): 11171.

[3] Cepa J J, Pavón R M, García-Alberti M, Caramés P. Towards BIM-GIS integration for road intelligent management system[J]. Journal of Civil Engineering and Management, 2023, 29(7): 621-638.

[4] Molina Andrés A A, Huang Y, Jiang Y. A review of unmanned aerial vehicle applications in construction management: 2016-2021[J]. Standards, 2023, 3(2): 95-109.

[5] Liang H, Lee S C, Bae W, Kim J, Seo S. Towards UAVs in construction: Advancements, challenges, and future directions for monitoring and inspection[J]. Drones, 2023, 7(3): 202.

[6] Kovanič Ľ, Topitzer B, Peťovský P, Blišťan P, Gergeľová M B, Blišťanová M. Review of photogrammetric and lidar applications of UAV[J]. Applied Sciences, 2023, 13(11): 6732.

[7] Kim Y H, Shin S S, Lee H K, Park E S. Field applicability of earthwork volume calculations using unmanned aerial vehicle[J]. Sustainability, 2022, 14(15): 9331.

[8] Chonpatathip S. Earthwork volume measurement in road construction using unmanned aerial vehicle (UAV)[J]. International Journal of Geoinformatics, 2023, 19(12): 51-64.

[9] Hasegawa H, Sujaswara A A, Kanemoto T, Tsubota K. Possibilities of using UAV for estimating earthwork volumes during process of repairing a small-scale forest road, case study from Kyoto Prefecture, Japan[J]. Forests, 2023, 14(4): 677.

[10] Muhammed S T, Abed F M. Combining terrestrial laser scanning and drone-based photogrammetry towards improving volume calculations in construction projects[J]. Journal of Engineering, 2025, 31(8): 26-50.

[11] Martínez-Carricondo P, Agüera-Vega F, Carvajal-Ramírez F. Accuracy assessment of RTK/PPK UAV-photogrammetry projects using differential corrections from multiple GNSS fixed base stations[J]. Geocarto International, 2023, 38(1): 2197507.

[12] Ersoz A B, Pekcan O. UAV-based automated earthwork progress monitoring using deep learning with image inpainting[J]. Automation in Construction, 2025, 175: 106211.

[13] Khan M S, Cho H S, Seo J. Voxel-based digital twin framework for earthwork construction[J]. Applied Sciences, 2025, 15(14): 7899.

[14] Cotoarbă D, Straub D, Smith I F C. Probabilistic digital twins for geotechnical design and construction[J]. Data-Centric Engineering, 2025, 6: e30.

[15] Li T, Rui Y, Zhao S, Zhang Y, Zhu H, Li X. A quantitative digital twin maturity model for underground infrastructure based on D-ANP[J]. Tunnelling and Underground Space Technology, 2024, 146: 105612.